Dynamic range of safe electrical stimulation of the retina

Alexander F. Butterwick[*1], Alexander Vankov[2,3], Phil Huie[2,3], Daniel V. Palanker[2,3]
[1]Department of Applied Physics, Stanford University, Stanford, CA
[2]Department of Ophthalmology, Stanford University School of Medicine, Stanford, CA
[3]Hansen Experimental Physics Labs, Stanford University, Stanford, CA

ABSTRACT

Electronic retinal prostheses represent a potentially effective approach for restoring some degree of sight in blind patients with retinal degeneration. However, levels of safe electrical stimulation and the underlying mechanisms of cellular damage are largely unknown. We measured the threshold of cellular damage as a function of pulse duration, electrode size, and number of pulses to determine the safe range of stimulation. Measurements were performed *in-vitro* on embryonic chicken retina with saline-filled glass pipettes for stimulation electrodes. Cellular damage was detected using Propidium Iodide fluorescent staining. Electrode size varied from 115μm to 1mm, pulse duration from 6μs to 6ms, and number of pulses from 1 to 7,500. The threshold current density was independent of electrode sizes exceeding 400μm. With smaller electrodes the current density was scaling reciprocal to the square of the pipette diameter, i.e. acting as a point source so that the damage threshold was determined by the total current in this regime. The damage threshold current measured with large electrodes (1mm) scaled with pulse duration as $t^{-0.5}$, which is characteristic of electroporation. For repeated electrical pulsed exposure on the retina the threshold current density varied between 0.059 A/cm2 at 6ms to 1.3 A/cm2 at 6μs. The dynamic range of safe stimulation, i.e. the ratio of damage threshold to stimulation threshold was found to be duration-dependent, and varied from 10 to 100 at pulse durations varying between 10μs to 10ms. Maximal dynamic range of 100 was observed near 1ms pulse durations.

Keywords: Retinal Prostheses, Propidium Iodide, Electrical Stimulation, Damage Threshold

1. Introduction

There is significant progress toward the development of an artificial retina. The realization of such a device aims to offer the first clinically effective treatment for many patients with age-related macular degeneration (AMD) and retinitis pigmentosa (RP). AMD is the major cause of vision loss in people over 65 in the Western world. Each year 700,000 people are diagnosed with AMD, and 10% of these people become legally blind[1]. RP occurs in about 1 out of 4000 live births, which corresponds to approximately 1.5 million people worldwide[2].

Both RP and AMD are characterized by degeneration of photoreceptors in the retina, yet it is understood that most of the afferent cellular network remains functional[3, 4]. The implants proposed by

[*] Communicating author: abutterw@stanford.edu, Hansen Experimental Physics Laboratory, Stanford University, 445 Via Palou, Stanford, California, 94305, phone (650) 723-0789

various groups are designed to provide visual perception by stimulating the preserved cells[5-7]. Acute and chronic electrical stimulation of the retina in patients with neuro-degenerative diseases using implanted arrays containing up to 16 electrodes has demonstrated the possibility of stimulating a perception of light, detection of motion and even simple shape discrimination[8, 9].

Electrical stimulation of neural cells is a profoundly fundamental and versatile therapeutic modality utilizing voltage sensititve ion channels and processes of electrical signaling intrinsic to many cells. Many electronic devices that interface with neural systems and electrically responsive tissues are already in clinical use. Examples of more common devices include deep brain stimulators for patients with Parkinson's and severe depression[10, 11], cochlear implants for patients with sensorineural hearing loss[12], and pacemakers for those suffering from a number of conduction irregularities in the heart[13]. All of these devices, along with retinal prostheses, expose functional and responsive tissues to supra-physiological levels of current injection and electric fields. Since these devices interface with healthy and functional systems for prolonged periods of time, it is paramount that cellular damage is avoided. Though previous studies have identified threshold levels of current or current density found to damage neural tissue, these investigations have been limited to only specific pulse durations, electrode sizes, and durations of exposure where the onset of cellular damage was seen relative to only one of the above parameters[14-18]. The understanding of retinal damage from electrical stimulation remains extremely limited. In fact, the work most commonly cited in the retinal prostheses community is a study by McCreery *et al.* involving chronic electrical stimulation of the cat cortex[14]. A more thorough exploration of the scaling of the damage threshold with these parameters will help in determining the optimal pulse duration for safe stimulation and perhaps elucidating mechanisms of cellular damage.

The investigation by McCreery *et al*[14]. established the current tenet in a series of experiments by electrically stimulating cat cortex *in-vivo* with charge balanced 400μs pulses at 50 Hz over the course of 7 hours. The investigators described tissue damage thresholds in terms of current density and total current using electrodes of various sizes. In one set of experiments charge injection was fixed at 1 mC/phase while the size of the electrode was varied. The authors determined the damage threshold charge density of 100 mC/cm^2 on an electrode size of 0.01 cm^2. In the second experiments, when the charge injection was varied on a fixed electrode size of 0.5 cm^2, damage was detected with a charge of 6 mC/phase and greater, corresponding to threshold charge density of 12 mC/cm^2. McCreery *et al.* concluded that the damage threshold is determined by the mutual contributions of charge per phase and charge density since neither charge per phase nor charge density were conserved between the two damage thresholds. To determine damage threshold scaling, Shannon extrapolated McCreery's results with an empirical model fit to McCreery's data[19]. However, there has been no experimental verification of the model and little physical justification was presented to validate the proposed scaling laws for arbitrary current injection or electrode size. There is even less understanding of how the damage threshold scales with pulse duration; in a manner analogous to the strength-duration curves of cellular stimulation[20-24]. As well as providing insight into cellular function and mechanisms, this would define the dynamic range of safe electrical stimulation of the retina and determine optimum operating parameters for an implanted device.

A need for a better understanding of the safe limits in acute and chronic electrical stimulation of biological tissue in general, and retinal tissue in particular, motivated this study. We explore the dependence of the damage threshold on electrode size, pulse duration, and number of pulses on excised retina.

2. METHODOLOGY

2.1 Tissue preparations

Retinal tissue for this study was harvested from chicken embryos (E15 - E19). For retinal preparations, the embryo was decapitated and the eye was removed. Within three minutes of euthanasia the eyecup was hemisected, the vitreous was removed, and the posterior portion of the eyecup was placed into DPBS. Once the retina began to separate from the retinal pigment epithelium, the choroid and scleara were removed from the now isolated retina. The retina was kept at room temperature in DPBS for stimulation, with the photoreceptors facing up, towards the stimulating electrodes. Each exposure of the electrical stimulus was done on a new, and healthy, region of the tissue.

2.2 Damage assay

Damaged cells were identified with propidium iodide staining, an assay used for dead-cell staining[25-27]. Propidium iodide is impermeable to normally functioning cell membranes. When propidium iodide binds to intracellular nucleic acids it becomes fluorescent; thus, it is used to identify abnormal permeability of the cellular membrane and disintegration of the nucleus. Roughly 100µL of propidium iodide (Sigma-Aldrich, MO) is mixed with the DPBS during damage assessment. The tissue was illuminated near the excitation wavelength of PI, 560nm, with a xenon lamp (XE-Lite, OTI, Toronto, Ontario) and appropriate filter (D540/25x, Chroma, VT), and imaged with a bandpass filter at the emission wavelength, 630nm (D630/60m, Chroma).

2.3 Electrical stimulation

To mitigate the possible effects of toxic electrochemical products being produced by high current densities on metal electrodes, saline filled glass pipettes were used with large surface-area platinum electrodes inside. The pipettes were pulled to aperture diameters from 100µm to 1 mm. Glass pipettes were verified as a good model system for planar disc electrodes by computer simulation (FEMLAB, Comsol, MA) of the field at the electrode surface with the typical edge enhancement of the electric field, Figure 1[28]. To accurately control pipette position and ensure apposition to the tissue surface, the pipette was controlled by a 3-dimensional micromanipulator, and monitored by two stereoscopes, one oriented normal to the surface and the second stereoscope at 60º to the tissue surface to ensure electrode apposition to the tissue.

Electrical pulses were biphasic with the cathodal phase first; both phases were created with independent monophasic pulse generators and were gated with a pulse generator (DG535, SRS, Sunnyvale, CA). The total current per phase was matched between the power supplies, and pipette impedance was measured with an oscilloscope. Pulse durations ranged from 6µs/phase – 6ms/phase, and number of pulses varied from 1 pulse to 7,500 pulses (25Hz for 5min.).

Since damage from cellular hyperthermia indistinguishable from electrical damage using the PI assay, it is important to verify that the stimulus is well below levels of thermal damage. Estimations of Joule heating are done following the methods of Palanker et al[29]. This estimates that from the applied currents no more than a 20mK temperature change can be attributed to the electrical exposure, which is well below thresholds of thermal damage.

3. RESULTS

Results from damage assessments are presented in terms of the maximal current density that consistently does not damage the retina, and the minimal current density levels that consistently damaged the retina. These two points are plotted in the following figures. Approximately five trials were taken at each of the threshold current densities plotted to ensure results were reproducible.

3.1 Number of pulses

The effect of multiple pulses in an acute *in-vivo* experiment is illustrated in Figure 2. In order to ensure accuracy, electrical exposure was always limited to a five-minute window and damage was assessed 15 minutes after exposure. PI uptake, and hence damaged cell fluorescence, is a time dependent process. At values near threshold, cellular repair processes and diffusion can quench the fluorescent signal, so despite abnormal cellular function, if samples are evaluated at different time points from electrical exposure it is possible to get erroneous assessments of damage. Therefore, as the number of pulses varied from 1 to 7,500, the repetition rate varied from 0 to 25 Hz. As can be seen from figure 2, threshold levels of electrical stimulation for a single electrical pulse are 7 times higher than levels of repeated stimulation. We define 7,500 as a chronic-type level of repeated stimulation. Damage thresholds reach levels of recurrent pulsing after only 50 pulses, a repetition rate of 0.17Hz. The damage threshold might further decrease as exposure of the tissue is extended for days, however this is not feasible for an *in-vitro* experiment especially when thresholds are a function of many parameters.

3.2 Pulse duration

Current density damage thresholds were taken with a 1mm pipette for single shot and 7,500 pulses. Data from this experiment is illustrated in Figure 3. The data obtained for chronic exposures is very close to data obtained from previous studies using a large pipette for 7 hours of stimulation[14]. However, this study explicitly looks at the scaling of current density with pulse duration. From Figure 4, it

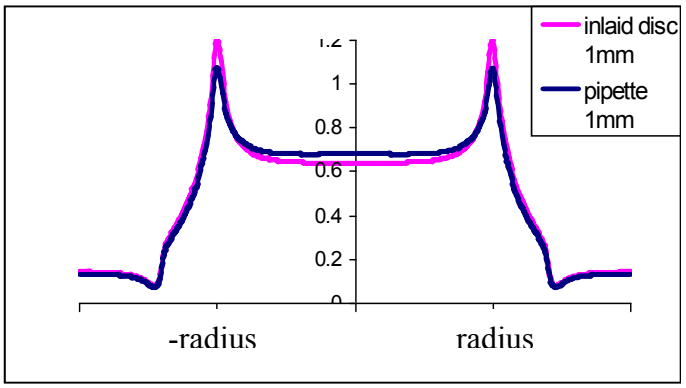

Figure 1. Comparison of electric field from an inlaid conductive disc and glass pipette. Edge enhancement is apparent at the edge of the conductive disc.[28]

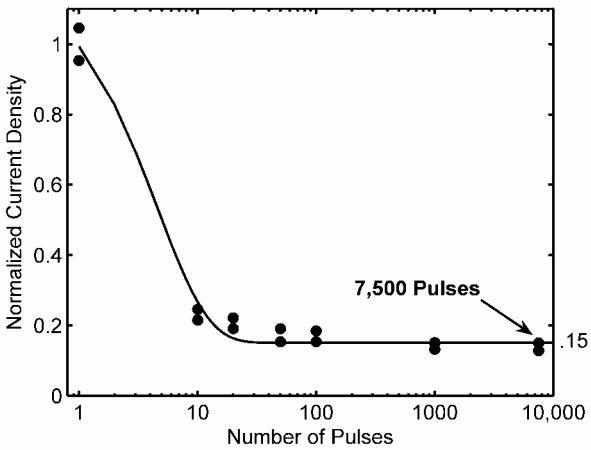

Figure 2. Repeated stimulation lowers damage thresholds significantly. Number of pulses in five minutes of exposure. The effect of repeated pulses in five minutes of exposure on levels of safe stimulation. Data taken represents thresholds for 60µs/phase pulses with a 1mm pipette on chick retina.

is seen that these thresholds scale approximately as $1/\sqrt{t}$, explicitly $t^{-0.48}$ for single shot and $t^{-0.41}$ for repeated exposures.

This implies that charge is not conserved along the strength duration curve. Scaling of current density with the inverse square root of pulse duration is characteristic of electroporation[30-32].

3.3 Electrode size

This study also attempts to thoroughly investigate current density thresholds as a function of electrode size. To understand the size dependence of electrodes on safe levels of damage 10 different sized pipettes ranging from 115um to 1mm were used. This data was taken with 60μs/phase pulse duration on the retina. From Figure 4 two regimes were made out. For large pipettes, the local field near the pipette approaches an infinite plane – here current density determines cellular damage. In fact, for pipettes larger than 500mm the current density threshold remains roughly constant. However, as the pipette becomes quite small, the current density scales as $1/r^2$, hence, total current is conserved.

To model the behavior of current density thresholds with variable electrode sizes it is necessary to calculate the current density at the cell under measurement, j_{cell}, for a given injection current j_0. If a disc electrode of radius r is a distance z from the cell, and we assume isotropic current flow, it can be shown that the injected current density depends on the local current density $j_0(z) = j_{cel}\dfrac{\sqrt{x^2+1}}{\sqrt{x^2+1}-1}$, where x=r/z. This model of the scaling is plotted as on figure 4 as the solid line. It is a good approximation of the scaling, but discrepancies between the data and the line are probably due to the fact the model doesn't take the electric field edge enhancement and tissue impedance into consideration. The data tends to reach the regime of current density conservation for large pipettes before the model.

3.4 Dynamic range of safe stimulation

Parameters of interest for the design and operation of retinal prostheses are electrode size and pulse duration. The general scaling of the damage and stimulation thresholds with the mentioned variables

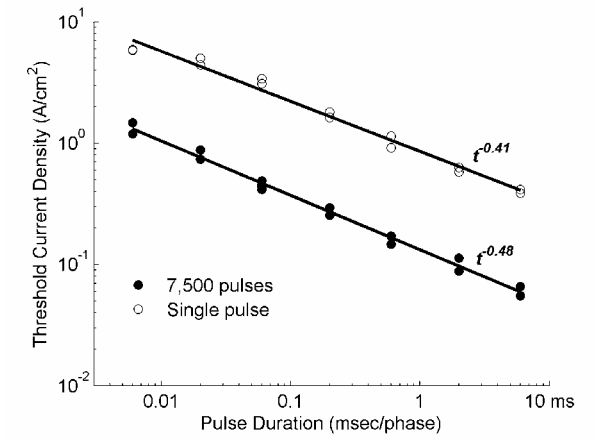

Figure 3. Scaling of current density damage threshold as a function of pulse length (per phase). Data taken using 1mm pipette with a single pulse and 7,500 pulses.

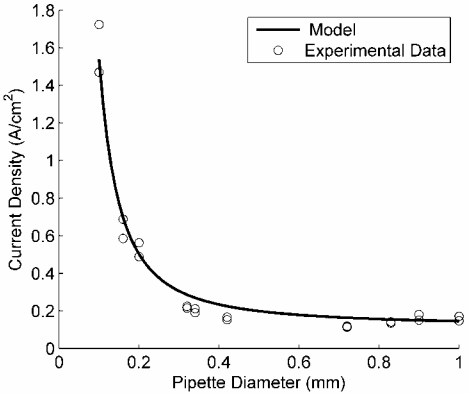

Figure 4. Dependence of threshold current density on electrode diameter. Data taken with 7,500 pulses of 60μs/phase in duration.

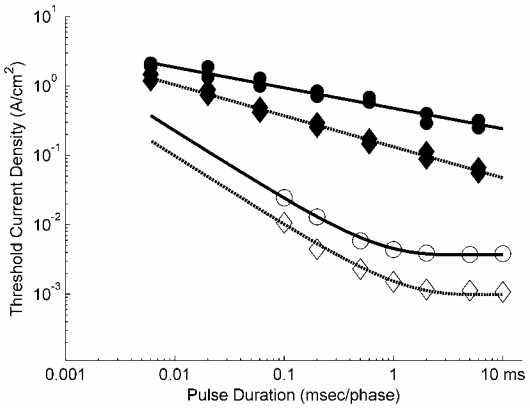

Figure 5. Damage threshold as a function of the pulse length (per phase) for 1mm diameter electrodes (♦) and 115µm diameter electrodes (●). For comparison, stimulation data is plotted for electrodes of similar diameters, 500µm (◊) and 120µm (o).

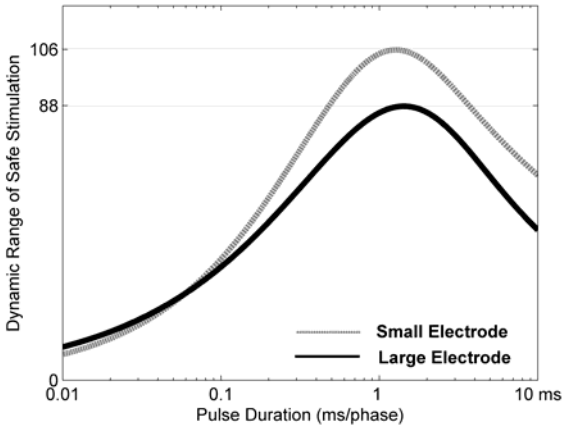

Figure 6. Ratio of the damage threshold to the stimulation threshold approximation shown in Figure 5. Maximal dynamic of safe stimulation occurs at roughly the chronaxie of the cells and is more dependent on pulse duration than electrode size.

provides guidance for the optimization of these parameters in order to achieve the larges possible dynamic range of safe stimulation for an electronic interface with the retina. Presented in figure 5 are results of the pulse length dependence on damage thresholds for large (1mm) and small (115µm) pipettes. It is apparent from Figure 5 that the scaling of damage thresholds is dependent on electrode size – current density for the larger electrodes scales as $t^{-0.45}$ while it scales as $t^{-0.29}$ for small electrodes. The data is also compared to *in-vitro* rabbit stimulation data generously provided by Dr. R. Jensen to estimate the dynamic range of safe stimulation. In Dr. Jensen's experiment small electrodes were 120µm in diameter and large electrodes were 500µm in diameter. Because of the results illustrated in Figure 4, there should be no difference in threshold current density between 500µm and 1mm electrodes. Dynamic range of safe stimulation of the retina (ratio of damage threshold to stimulation threshold) appears to be strongly dependent on pulse duration, but only weakly tied to electrode size, Figure 6. The pulse duration of maximal dynamic range is near chronaxie, approximately 1.3ms. From this data the maximum dynamic range is roughly 100, this is more than sufficient for the stimulation of neural cells with a typical linear range of ~30 [33, 34].

4. CONCLUSION

This study investigated the dependence of current density damage thresholds on electrode size and pulse duration of repeated pulsed electrical stimulation on chick retina. The study was designed to delineate parameters of safe electrical stimulation of the retina towards the development of prosthetic devices. For electrodes with a diameter greater than 400µm, i.e. large compared to cellular lengths and the separation between cells and the electrode, damage is determined by the injected *current density*. For small electrodes, as the electrode approaches a point source compared to the distance from the tissue, the *total current* determines damage. Damage threshold current density scales with pulse duration for large electrodes approximately as $1/t^{0.5}$. Damage thresholds decrease 0.15 times single pulse levels when the pulse is repeated more than 50 times.

Acknowledgements

The authors would like to thank Itzhak Hakim, Yev Freyvert, Erik Anderson, and Naomi Palanker for their help in establishing portions of the experiments. Thanks to Ralph Jensen for supplying stimulation data used for comparison. Funding was provided by the MFEL grant from the Air Force Office of Scientific Research.

References

1. Curcio, C.A., N.E. Medeiros, and C.L. Millican, *Photoreceptor loss in age-related macular degeneration.* Investigative Ophthalmology & Visual Science, 1996. 37(7): p. 1236-49.
2. Berson, E.L., et al., *Vitamin A supplementation for retinitis pigmentosa.* Arch Ophthalmol, 1993. 111(11): p. 1456-9.
3. Santos, A., et al., *Preservation of the inner retina in retinitis pigmentosa. A morphometric analysis.* Archives of Ophthalmology, 1997. 115(4): p. 511-5.
4. Stone, J.L., et al., *Morphometric analysis of macular photoreceptors and ganglion cells in retinas with retinitis pigmentosa.* Archives of Ophthalmology, 1992. 110(11): p. 1634-9.
5. Wyatt, J. and J. Rizzo, *Ocular implants for the blind.* Ieee Spectrum, 1996. 33(5): p. 47-&.
6. Liu, W., et al., *The engineering of a prototype retinal prosthesis.* Investigative Ophthalmology & Visual Science, 1999. 40(4): p. S782-S782.
7. Normann, R.A., et al., *A neural interface for a cortical vision prosthesis.* Vision Research, 1999. 39(15): p. 2577-87.
8. Humayun, M., et al., *Chronically implanted intraocular retinal prosthesis in two blind subjects.* Investigative Ophthalmology & Visual Science, 2003. 44: p. U467-U467.
9. Humayun, M.S., et al., *Visual perception elicited by electrical stimulation of retina in blind humans.* Archives of Ophthalmology, 1996. 114(1): p. 40-46.
10. Lozano, A.M., et al., *Deep brain stimulation for Parkinson's disease: disrupting the disruption.* Lancet Neurol, 2002. 1(4): p. 225-31.
11. Mayberg, H.S., et al., *Deep brain stimulation for treatment-resistant depression.* Neuron, 2005. 45(5): p. 651-60.
12. Miyamoto, R.T., et al., *Cochlear implantation in auditory neuropathy.* Laryngoscope, 1999. 109(2 Pt 1): p. 181-5.
13. Boriani, G., et al., *Clinical relevance of atrial fibrillation/flutter, stroke, pacemaker implant, and heart failure in Emery-Dreifuss muscular dystrophy: a long-term longitudinal study.* Stroke, 2003. 34(4): p. 901-8.
14. McCreery, D.B., et al., *Charge density and charge per phase as cofactors in neural injury induced by electrical stimulation.* IEEE Transactions on Biomedical Engineering, 1990. 37(10): p. 996-1001.
15. Asanuma, H. and A.P. Arnold, *Noxious effects of excessive currents used for intracortical microstimulation.* Brain Res, 1975. 96(1): p. 103-7.
16. Sambelashvili, A.T., V.P. Nikolski, and I.R. Efimov, *Virtual electrode theory explains pacing threshold increase caused by cardiac tissue damage.* Am J Physiol Heart Circ Physiol, 2004. 286(6): p. H2183-94.
17. Gekeler, F., et al., *Subretinal electrical stimulation of the rabbit retina with acutely implanted electrode arrays.* Graefes Archive for Clinical and Experimental Ophthalmology, 2004. 242(7): p. 587-596.
18. Yamauchi, Y., et al. *Subretinal Placement of the Microelectrode Array Is Associated With a Low Threshold for Electrical Stimulation.* in *Annual Meeting of the Association for Research in Vision and Ophthalmology*. 2005. Fort Lauderdale, Florida: Investigative Ophthalmology & Visual Science.
19. Shannon, R.V., *A model of safe levels for electrical stimulation.* IEEE Transactions on Biomedical Engineering, 1992. 39(4): p. 424-6.
20. Mogyoros, I., M.C. Kiernan, and D. Burke, *Strength-duration properties of human peripheral nerve.* Brain, 1996. 119: p. 439-447.
21. Jensen, R.J., et al., *Thresholds for activation of rabbit retinal ganglion cells with an ultrafine, extracellular microelectrode.* Investigative Ophthalmology & Visual Science, 2003. 44(8): p. 3533-43.
22. Jensen, R.J., O.R. Ziv, and J.F. Rizzo, 3rd, *Thresholds for activation of rabbit retinal ganglion cells with relatively large, extracellular microelectrodes.* Investigative Ophthalmology & Visual Science, 2005. 46(4): p. 1486-96.

23. Roth, B.J., *A Mathematical-Model of Make and Break Electrical-Stimulation of Cardiac Tissue by a Unipolar Anode or Cathode.* Ieee Transactions on Biomedical Engineering, 1995. 42(12): p. 1174-1184.
24. Roth, B.J., *Mechanisms for Electrical-Stimulation of Excitable Tissue.* Critical Reviews in Biomedical Engineering, 1994. 22(3-4): p. 253-305.
25. Belloc, F., et al., *A flow cytometric method using Hoechst 33342 and propidium iodide for simultaneous cell cycle analysis and apoptosis determination in unfixed cells.* Cytometry, 1994. 17(1): p. 59-65.
26. Bevensee, M.O., C.J. Schwiening, and W.F. Boron, *Use of BCECF and propidium iodide to assess membrane integrity of acutely isolated CA1 neurons from rat hippocampus.* Journal of Neuroscience Methods, 1995. 58(1-2): p. 61-75.
27. Wilde, G.J., L.E. Sundstrom, and F. Iannotti, *Propidium iodide in vivo: an early marker of neuronal damage in rat hippocampus.* Neuroscience Letters, 1994. 180(2): p. 223-6.
28. Mierisch, A.M., S.R. Taylor, and V. Celli, *Understanding the degradation of organic coatings through local electrochemical impedance methods - II. Modeling and experimental results of normal field variations above disk electrodes.* Journal of the Electrochemical Society, 2003. 150(7): p. B309-B315.
29. Palanker, D., I. Turovets, and A. Lewis, *Electrical alternative to pulsed fiber-delivered lasers in microsurgery.* Journal of Applied Physics, 1997. 81(11): p. 7673-7680.
30. Neumann, E., *Membrane Electroporation and Direct Gene-Transfer.* Bioelectrochemistry and Bioenergetics, 1992. 28(1-2): p. 247-267.
31. Neumann, E., et al., *Mechanism of electroporative dye uptake by mouse B cells.* Biophysical Journal, 1998. 74(1): p. 98-108.
32. Neumann, E., K. Tonsing, and P. Siemens, *Perspectives for microelectrode arrays for biosensing and membrane electroporation.* Bioelectrochemistry, 2000. 51(2): p. 125-32.
33. Yang, X.L. and S.M. Wu, *Response sensitivity and voltage gain of the rod- and cone-bipolar cell synapses in dark-adapted tiger salamander retina.* Journal of Neurophysiology, 1997. 78(5): p. 2662-73.
34. Berntson, A. and W.R. Taylor, *Response characteristics and receptive field widths of on-bipolar cells in the mouse retina.* Journal of Physiology, 2000. 524 Pt 3: p. 879-89.